

Molecular BioSystems

Accepted Manuscript



This is an *Accepted Manuscript*, which has been through the Royal Society of Chemistry peer review process and has been accepted for publication.

Accepted Manuscripts are published online shortly after acceptance, before technical editing, formatting and proof reading. Using this free service, authors can make their results available to the community, in citable form, before we publish the edited article. We will replace this *Accepted Manuscript* with the edited and formatted *Advance Article* as soon as it is available.

You can find more information about *Accepted Manuscripts* in the [Information for Authors](#).

Please note that technical editing may introduce minor changes to the text and/or graphics, which may alter content. The journal's standard [Terms & Conditions](#) and the [Ethical guidelines](#) still apply. In no event shall the Royal Society of Chemistry be held responsible for any errors or omissions in this *Accepted Manuscript* or any consequences arising from the use of any information it contains.



www.rsc.org/molecularbiosystems

Mathematical modeling deciphers the benefits of alternatively-designed conserved activatory and inhibitory gene circuits

Ahmet Ay

Departments of Biology and Mathematics, Colgate University
13 Oak Dr. Hamilton, NY 13346

Natalie Wilner

Department of Biology, Colgate University
13 Oak Dr. Hamilton, NY 13346

Necmettin Yildirim*

Division of Natural Sciences, New College of Florida
5800 Bayshore Road, Sarasota, FL 34243

April 30, 2015

Abstract

Cells employ a variety of mechanisms as a response to external signals to maintain cellular homeostasis. In this study, we examine four activatory and four inhibitory protein synthesis mechanisms at both population and single cell level that can be triggered by a transient external signal. Activation mechanisms result from the assumption that cells can employ four different modes to temporarily increase the levels of a protein: decreased mRNA degradation, increased mRNA synthesis, decreased protein degradation and increased protein synthesis. For the inhibition mechanisms it is assumed that a cell can reduce a protein's level through four ways: increased mRNA degradation, reduced mRNA synthesis, increased protein degradation and reduced protein synthesis.

*Corresponding author: E-mail addresses: nyildirim@ncf.edu, tel: (941) 487-4214; fax: (941) 487-4396;

Deterministic and stochastic models were developed to analyze the dynamic responses of these eight mechanisms to a transient signal. Three different response metrics were used to measure different aspects of the response. These metrics are (i) mid-protein abundance (mP), (ii) time required for the protein to reach the mid-protein level (mT), and (iii) duration of response (D), which is defined as the total time for which the protein (P) abundance are above or below of mid-protein level. Our simulations show that of the activation mechanisms, the signal-dependent increase in mRNA synthesis and protein synthesis are more effective and faster, than the signal dependent decrease in mRNA and protein degradation. On the other hand, the mechanism involving signal dependent increase in protein synthesis is noisier than the signal dependent increase in mRNA synthesis in regard to all metrics used. Of the four inhibition mechanisms, the signal-dependent increase in the protein degradation is the most effective and fastest of the four inhibition mechanisms. It is also noisiest of the four inhibition mechanisms before the protein levels reach a steady state around 100 minutes.

Keywords: Mathematical modeling, deterministic simulation, stochastic simulation, signal transduction, gene circuit, network motifs

1 Introduction

Cells utilize a variety of mechanisms to regulate gene expression. As dictated by the central dogma of molecular biology, cells replicate their DNA, DNA is transcribed into mRNA, and then mRNA is translated into protein, which results in an increase in protein abundance[1]. Cells use multiple ways to regulate the abundance of a protein. At the chromosome level, DNA is wrapped around histone proteins into chromatin, and it is only expressed when it is in the decondensed state [2, 3, 4]. Transcription factors bind to DNA to help activate transcription in both prokaryotes and eukaryotes [5, 6, 7]. After transcription initiation, the regulation processes are similar in prokaryotes and eukaryotes [8]. For transcriptional elongation to occur, elongation factors bind DNA to overcome RNA Polymerase II pause, arrest, and termination, and the binding of these factors thus presents further opportunities for transcriptional regulation [9]. In eukaryotes, mRNA processing allows for further regulation during transcription, including the addition of a 5' cap which enhances mRNA stability[10, 11, 12], a poly-A tail to the 3' end of the mRNA [13], and alternative splicing[10]. There are multiple ways for a cell to reduce the levels of an mRNA transcript, including, deadenylation, decapping, endonucleolytic cleavage[14, 15, 11], as well as miRNA-induced degradation [16]. When, mRNA undergoes translation to form protein, protein degradation can occur through multiple mechanisms, including ubiquitination [17] and proteasome ac-

tivity such as the 26S proteasome [18]. These different layers of regulation give rise to the complexity of gene expression. Biological systems can be studied through experimentation, but because of their great complexity, this could be challenging, if not impossible. Therefore, mathematical modeling provides great opportunity to study such complex biological systems *in silico*.

Gene regulation is an area of active research in the avenue to better understand the activation and inhibition of transcription, translation, and degradation of synthesized products. Some of the possible mechanisms of regulation include negative autoregulation, positive autoregulation, as well as feed-forward loops [19]. It has been demonstrated that although gene regulatory networks with different underlying architecture can result in similar dynamics, the architecture is very important in terms of how that system functions under different conditions[20]. Studying small-scale gene regulatory networks provides the chance to understand the physiological roles of specific network architectures[21, 22, 23].

Here we explore four different activation and four distinct inhibition mechanisms that respectively increase and decrease cellular protein levels as a response to a signal. These mechanisms are shown in Figure 1. The systems are modeled using generic mRNA(M) and protein(P) that hinge on the relationship between the synthesis and degradation rates. A transient signal is used to perturb these eight mechanisms when they are at a resting state. We examine how changes in the signal amplitude and persistency affect the protein expression levels, which are measured by three response metrics that characterize different aspect of protein dynamics.

As response metrics, we use mid-protein abundance (mP), time required for the protein to reach this level (mT), and duration of response (D). The duration of the response D is defined as the total time for which the protein (P) levels are below (for inhibition mechanisms) or above (for activation mechanisms) of its mid-protein level. These metrics are depicted in Figure 2.

2 Mathematical Models

The mathematical models presented in this study describe eight different mechanisms shown in Figure 1 to regulate a generic protein (P) through a transient signal $S(t)$. To study average dynamic responses of these regulatory mechanisms, we have devised simple ordinary differential equation(ODE) models according to mass-action kinetics. The models utilize common parameters although they differ in their mechanisms and therefore in their equations. These mechanisms represent a variety of ways in which a cell can increase or decrease

protein abundance through affecting mRNA(M) or protein(P) synthesis or degradation. For practical purposes, some abbreviations are used in naming the mechanisms. In a mechanism name, A stands for activation, I stands for inhibition, m represents mRNA and p represents the protein. The letters s and d respectively denote regulations at the synthesis and degradation steps. The sign $+$ represents increase and $-$ represents decrease in synthesis or degradation steps. For example, mechanism A_{md-} is the the activation mechanism and the activation is due to a decrease in mRNA degradation. The activation mechanisms all represent different ways to increase protein abundance in a cell. Similarly, mechanism I_{pd+} is the the inhibition mechanism and the inhibition is due to an increase in protein degradation rate. The inhibitory mechanisms demonstrate various ways to decrease protein abundance in a cell.

===== Figure 1 here =====

In all the models, the net rate of change in the mRNA abundance($\frac{dM}{dt}$) is assumed to be the difference of its mRNA synthesis and degradation rates as in Eq.(1). The net rate of change in the protein abundance($\frac{dP}{dt}$) is assumed to be the difference between its protein synthesis and degradation rates and can be modelled by Eq.(2).

$$\frac{dM}{dt} = \alpha_m - \beta_m M \quad (1)$$

$$\frac{dP}{dt} = \alpha_p M - \beta_p P \quad (2)$$

In this simplistic model, the mRNA synthesis rate is assumed to be constant (α_m) and its degradation rate ($\beta_m M$) is assumed to be a linear function of the mRNA abundance. The protein production rate is taken as a linear function of the mRNA abundance ($\alpha_p M$) and its degradation rate is assumed to be a linear function of protein abundance ($\beta_p P$). To explore the signal dependent responses of the simple regulatory activation mechanisms, we multiply α_m and $\alpha_p M$ by $1 + S(t)$ to increase synthesis rates, or divide $\beta_m M$ and $\beta_p P$ by $1 + S(t)$ to decrease degradation rates. Similarly, to study the simple regulatory inhibition mechanisms, we divide the rate of production α_m and $\alpha_p M$ by $1 + S(t)$ or multiply the rate of degradation $\beta_m M$ and $\beta_p P$ by $1 + S(t)$.

For example, to model a signal-induced activation mechanism, the mRNA(M) synthesis rate α_m can be multiplied by $1 + S(t)$ to reflect an increased mRNA synthesis rate. This mechanism is shown as mechanism A_{ms+} in Figure 1, whose dynamic response is modeled by Eqs.(3) and (4)

$$\frac{dM}{dt} = \alpha_m(1 + S(t)) - \beta_m M \quad (3)$$

$$\frac{dP}{dt} = \alpha_p M - \beta_p P \quad (4)$$

It is to note that in the absence of the signal, all our models yield a nonzero stable steady state for the mRNA and protein abundance at $(M^*, P^*) = \left(\frac{\alpha_m}{\beta_m}, \frac{\alpha_m \alpha_p}{\beta_m \beta_p}\right)$.

===== Figure 2 here =====

The time dependent signal profile $S(t)$ is assumed to be a step function with two parameters γ and k , and it has the following form

$$S(t) = \begin{cases} \gamma, & \text{if } 0 \leq t < k \\ 0, & \text{if } t \geq k \end{cases} \quad (5)$$

The signal amplitude parameter (γ) measures the system's sensitivity to the perturbation caused by the signal, and the signal persistency parameter (k) controls how long the signal is applied to the system.

2.1 The Activation Mechanisms

The four differential equation systems listed in Table 1 model the signal induced activation mechanisms.

Table 1: The model equations for four different activation mechanisms A_j for $j = \{md^-, ms^+, pd^-, ps^+\}$

$$A_{md^-}: \begin{cases} \frac{dM}{dt} = \alpha_m - \frac{\beta_m}{1+S(t)} M \\ \frac{dP}{dt} = \alpha_p M - \beta_p P \end{cases} \quad A_{ms^+}: \begin{cases} \frac{dM}{dt} = \alpha_m(1 + S(t)) - \beta_m M \\ \frac{dP}{dt} = \alpha_p M - \beta_p P \end{cases}$$

$$A_{pd^-}: \begin{cases} \frac{dM}{dt} = \alpha_m - \beta_m M \\ \frac{dP}{dt} = \alpha_p M - \frac{\beta_p}{1+S(t)} P \end{cases} \quad A_{ps^+}: \begin{cases} \frac{dM}{dt} = \alpha_m - \beta_m M \\ \frac{dP}{dt} = \alpha_p(1 + S(t))M - \beta_p P \end{cases}$$

In mechanism (A_{md^-}), the transient increase in the protein level is due to a decrease in the mRNA degradation rate. In mechanism (A_{ms^+}), it is assumed that the increase in the protein abundance is due to a signal-induced increase in the mRNA synthesis rate. In

mechanism (A_{pd-}), the transient increase in the protein level is caused by a decrease in the protein degradation rate. In mechanism (A_{ps+}), the assumption is that the increase in the protein abundance is a result of a signal-induced increase in the protein synthesis rate. The model in A_{md-} includes the basal mRNA and protein synthesis rates α_m and $\alpha_p M$, and the basal protein degradation rate $\beta_p P$ along with an mRNA degradation rate $\beta_m M$, which is negatively regulated by the signal $S(t)$. A similar approach can be used to describe the other activation mechanisms.

2.2 The Inhibition Mechanisms

The system of differential equations in Table 2 describe four different signal mediated transient inhibitions of the protein abundance.

Table 2: The models for the inhibition mechanisms I_j for $j = \{md^+, ms^-, pd^+, ps^-\}$

$$\begin{aligned}
 I_{md^+} : \quad & \begin{cases} \frac{dM}{dt} = \alpha_m - \beta_m(1 + S(t))M \\ \frac{dP}{dt} = \alpha_p M - \beta_p P \end{cases} & I_{ms^-} : \quad & \begin{cases} \frac{dM}{dt} = \frac{\alpha_m}{1+S(t)} - \beta_m M \\ \frac{dP}{dt} = \alpha_p M - \beta_p P \end{cases} \\
 I_{pd^+} : \quad & \begin{cases} \frac{dM}{dt} = \alpha_m - \beta_m M \\ \frac{dP}{dt} = \alpha_p M - \beta_p(1 + S(t))P \end{cases} & I_{ps^-} : \quad & \begin{cases} \frac{dM}{dt} = \alpha_m - \beta_m M \\ \frac{dP}{dt} = \frac{\alpha_p}{1+S(t)}M - \beta_p P \end{cases}
 \end{aligned}$$

In mechanism (I_{md+}), the transient decrease in the protein level is due to an increase in the mRNA degradation rate. In mechanism (I_{ms-}), the decrease in the protein abundance is a result of a signal-dependent decrease in the mRNA synthesis rate. In mechanism (I_{pd+}), the transient reduction in the protein level is due to a faster protein degradation rate. In mechanism (I_{ps-}), the decrease in the protein abundance is due to a signal-induced inhibition of the protein synthesis rate. The model in I_{md+} involves the basal mRNA and protein synthesis rates, α_m and $\alpha_p M$, and basal protein degradation rate $\beta_p P$ along with a mRNA degradation rate, $\beta_m M$, which is increased by the signal $S(t)$. Similar descriptions apply to the other three inhibition models.

2.3 Parameter Values

To make this study more biologically realistic, the model parameters are collected or estimated from the literature for *E. coli*. In this section, the details of how the parameter values

used here have been estimated.

- β_m : The median mRNA half life has been measured for *E. coli* as 3.69 ± 0.49 [24]. In a more recent study, the average mRNA half life is estimated as 5-10 minutes [25]. We used 5 minutes for the mRNA half-life in this study. Assuming the degradation occurs exponentially, this figure gives an estimate of $\frac{\ln(2)}{5} = 0.1386 \text{ min}^{-1}$ for the mRNA degradation parameter β_m .
- α_m : mRNA copy number per cell in *E. coli* shows variation, which are experimentally measured to be between 0.1 and 60 mRNA molecules per cell [26]. In another recent study, quantitative system wide measurements of mRNA and protein levels in individual cells using single-molecule counting technique have been used. This study showed that mRNA copy number per cell ranges from 10^{-3} to 10 (Taniguchi *et al.* 2010). Here we took the steady state level of 4 mRNA molecules per cell. From Eq.(1), the steady state M^* becomes $M^* = \frac{\alpha_m}{\beta_m}$, which provides an estimate of 0.5544 molecules per minute for α_m .
- β_p : The protein half-life changes from protein to protein and between 15 and 120 minutes in *E. coli* [27]. Assuming the temporal degradation profile is exponential, these two figures give two estimates of 0.0462 and 0.0057 min^{-1} for the degradation rate parameter β_p . Here, we used 0.02 min^{-1} for this parameter, which is approximately equal to the average of these two numbers and provides a half-life of 35 minutes for the protein.
- α_p : Ishihama *et al.* [28] experimentally studied the protein abundances in *E. coli* and classified all proteins of *E. coli* into three groups and reported that the average number of protein molecules per gene as 500. By Eq.(2), the steady state equation for the protein becomes $\alpha_p M^* = \beta_p P^*$, which leads to an estimate for the parameter α_p as $\alpha_p = \frac{\beta_p P^*}{M^*} = 2.5$ per minute in the absence of signal. This estimate was used in our deterministic simulations. To study the effects of noise and cell-to-cell variation on the system dynamics, we used $\alpha_p = 0.5 \text{ molec/minute}$ in our stochastic simulations, which provides a steady state molecule number of $P^* = \frac{M^* \alpha_p}{\beta_p} \approx \frac{4 \times 0.5}{0.02} = 100 \text{ molec/cell}$ for the protein.
- k : This parameter is used to mimic the signal persistency. The smaller values of this parameter indicate a less persistent signal whereas the larger values of this parameter represent a more persistent and prolonged signal. The value of this parameter changes from 5 to 100 minutes in the deterministic simulations. To study the effect of noise

on the system dynamics, we used a transient signal profile with $k = 100$ minutes in the stochastic simulations.

- γ : This parameter refers to the signal amplitude, which measures system's sensitivity to the signal. We varied this parameter from 1 to 20, resulting in up to a 21 fold change in the production/degradation rates in the deterministic simulations. For the stochastic simulations, we fixed this parameter at $\gamma = 20$.

3 The Results for the Activation Mechanisms

For the deterministic simulations, the mathematical models given in Table 1 were numerically solved in **MatLab** for the parameter values provided in Section 2.3. In these simulations, the signal persistency parameter k is varied between 5 and 100 minutes, and the signal amplitude parameter γ is changed between 1 and 20. Then the changes in the response metrics are summarized in Sections 3.1 - 3.4.

3.1 Comparison of the mRNA Control Mechanisms

To study the effect of the transient signal on the protein abundance in two distinct mRNA targeted regulatory mechanisms, we numerically solved the model equations for mechanisms A_{md-} , decreased mRNA degradation rate, and mechanism A_{ms+} , increased mRNA synthesis rate. Both of these mechanisms result in an increase in protein abundance, but they employ distinct regulatory mechanisms to accomplish this result. Our simulation results show that increasing the mRNA production rate (A_{ms+}) produces higher mP than decreasing the mRNA degradation rate (A_{md-}) (Figure 3A). In addition, mechanism A_{ms+} is faster than mechanism A_{md-} (Figure 3B). But, the duration for both mechanisms is comparable (Figure 3C).

===== Figure 3 here =====

As a response to a 21 fold increase in the signal amplitude with a persistent signal (k is large), the mid-protein abundance mP increases up to 2037 molec/cell in mechanism A_{md-} as opposed to 4724 molec/cell for mechanism A_{ms+} . This suggests about ~ 2.3 fold difference in the mid-protein mP values between the two mechanisms for this signal profile. The same signal profile produces ~ 4.1 fold increase in mechanism A_{md-} compared to ~ 9.5 fold increase in mechanism A_{ms+} from the steady state level of 500 molec/cell. In mechanism A_{md-} , when signal amplitude $\gamma > \sim 5$, the signal persistency k has a significant effect on mP levels. The γ value has to be greater than ~ 12.5 to observe a similar effect

in the A_{ms+} mechanism. When the signal amplitude γ is fixed at a high value, as the signal persistence increases (for $k > \sim 40$), there is slightly less variation in mechanism A_{ms+} than the variation in mechanism A_{md-} for the metric mP . But, at a fixed value for signal persistency k , there is slightly more variation in mechanism A_{ms+} than in mechanism A_{md-} . In regards to the metric mT , mechanism A_{ms+} is quicker than A_{md-} , with a maximum mT of 36 min compared to 63 min. Qualitatively the heat maps for the mT and D of these two mechanisms are relatively similar. However, it should be noted that for a fixed signal persistency as the signal amplitude increases, mechanism A_{ms+} does not show variation in mT and D levels but mechanism A_{md-} shows slight variations.

3.2 Comparison of the Protein Control Mechanisms

To study the effect of the transient signal on the protein abundance P in two distinct protein targeted regulatory mechanisms, we employed the decreased protein degradation rate, mechanism A_{pd-} , and increased protein synthesis rate, A_{ps+} . Both mechanisms promote increases in P levels in cells, but they make use of distinct regulatory mechanisms. To simulate the systems, we numerically solved the model equations for A_{pd-} and A_{ps+} for the parameter values listed in Section 2.3 as γ and k change. Our simulations predict that increasing the production rate (mechanism A_{ps+}) is more effective in increasing mP levels (Figure 3A). For persistent and high amplitude signals ($\gamma = 20$ and $k = 100$), in mechanism A_{pd-} protein levels can go up to an average of 957 molec/cell (~ 1.9 fold of the steady state level), but in mechanism A_{ps+} the mid-protein levels can increase up to 4803 molec/cell (~ 9.6 fold of the steady state level). This suggests that mechanism A_{ps+} can increase mP levels ~ 5 fold more than mechanism A_{pd-} .

Further, mP dependency on signal persistency and amplitude in mechanisms A_{pd-} and A_{ps+} is significantly different. For a certain value of signal persistency, mechanism A_{pd-} has less variation compared to mechanism A_{ps+} . However, for a fixed value of the signal amplitude, the opposite behavior is observed. This suggests that varying signal amplitude leads to a higher variation in protein abundance in mechanism A_{ps+} but a similar behavior can be obtained using mechanism A_{pd-} by varying the signal persistency parameter k . But, it is important to emphasize that the protein abundance is significantly greater in mechanism A_{ps+} compared to mechanism A_{pd-} .

On the other hand, A_{pd-} and A_{ps+} mechanisms show qualitatively similar dynamics in the mT values (time needed to reach mid-protein level) as the signal persistency and signal amplitude change (Figure 3B). Despite this qualitative similarity, mechanism A_{ps+} shows a quicker response. In both mechanisms A_{pd-} and A_{ps+} for a fixed signal persistency k , mT

does not change significantly as signal amplitude γ increases. However, for both mechanisms, when signal amplitude γ is held constant, mT values increase as the signal persistency k increases. With regards to the third metric D , our numerical simulations show that the mechanisms A_{pd-} and A_{ps+} exhibit similar qualitative and quantitative behaviors on the duration metric D (Figure 3C).

3.3 Comparison of the mRNA versus Protein Control Mechanisms

Overall, the mRNA and protein synthesis mechanisms show qualitatively similar behavior (Figure 3A). For persistent and high amplitude signal ($\gamma = 20$ and $k = 100$), mechanism A_{ms+} (increase in mRNA synthesis) leads to an average mP level of 4724 molec/cell, while mechanism A_{ps+} (increase in protein production) results in an average mP level of 4803 molec/cell. This is ~ 9.5 and ~ 9.6 fold increase from steady state levels, respectively. In regards to the mT metric (Figure 3B), mechanism A_{ps+} shows slightly faster response compared to mechanism A_{ms+} (29 min and 36 min respectively). Although mechanism A_{ps+} results in slightly higher mid-protein levels in a quicker time, the difference is small. In addition, the duration of the response D is similar in both mechanisms (Figure 3C).

In comparing the inhibition of mRNA degradation (A_{md-}) and inhibition of protein degradation (A_{pd-}) mechanisms, mechanism A_{md-} is more efficient than mechanism A_{pd-} . For persistent and high amplitude signal, mechanism A_{md-} results in mP levels of 2037 molec/cell whereas mechanism A_{pd-} results in mP levels of 957 molec/cell (~ 4.1 fold increase compared to ~ 1.9 fold increase from steady state levels, respectively) (Figure 3A). The difference between these two mechanisms in regards to the minimum time to reach the mid-protein level mT is $\sim 28\%$ (63 min in A_{md-} vs 49 min in A_{pd-}) (Figure 3B). On the other hand, the duration metric D has similar behavior for these two mechanisms (103 min and 98 min) (Figure 3C).

3.4 Comparison of the Synthesis versus Degradation Mechanisms

In looking at the simulation results together, for a persistent and strong signal profile, the mechanisms that increase the mRNA and protein synthesis, A_{ms+} and A_{ps+} , are more effective in increasing mP level (4724 molec/cell and 4803 molec/cell vs. 2037 molec/cell and 957 molec/cell) and quicker (36 min and 29 min vs. 63 min and 49 min) than the mRNA and protein degradation mechanisms, A_{md-} and A_{pd-} . But, duration for all mechanisms is comparable, although mechanisms A_{ms+} and A_{ps+} show slightly longer durations (109 min and 108 min, respectively) compared to A_{md-} and A_{pd-} (103 min and 98 min, respectively).

Of all four mechanisms, A_{pd-} is the least effective and A_{md-} is the slowest. Furthermore, changes in the signal amplitude have almost no effect on the protein abundance when $\gamma > \sim 5$ in mechanism A_{pd-} . But, the other mechanisms show greater dependence on both γ and k . The heat maps for mechanisms A_{ms+} and A_{ps+} are qualitatively similar. It seems that the high mid-protein levels can only be reached when the signal amplitude $\gamma > \sim 10$ and signal persistency k is large enough.

4 The Results for the Inhibition Mechanisms

In Sections 4.1 - 4.4, we summarize how the response metrics change as the signal profile changes in the deterministic models for the inhibition mechanisms.

4.1 Comparison of the mRNA Control Mechanisms

To study the effect of the transient signal on the protein abundance in two distinct mRNA targeted regulatory mechanisms, the model equations for mechanisms I_{md+} (increased mRNA degradation rate) and I_{ms-} (decreased mRNA synthesis rate) were solved numerically. Through distinct regulatory mechanisms, both of these mechanisms result in a decrease in protein abundance. Our numerical simulations predict that I_{md+} results in comparable mP abundance to I_{ms-} (Figure 4A) and displays similar mT and D values (Figure 4B and C).

===== Figure 4 here =====

As a response to a 21 fold increase in the signal amplitude with a persistent signal (k is large), the mP decreases down to 295 molec/cell in mechanism I_{md+} as opposed to 299 molec/cell in mechanism I_{ms-} . These mP levels are ~ 1.7 fold lower than the steady state level 500 molec/cell. Qualitatively, both mechanisms have similar heat maps for mP metric. For the signal profiles with fixed persistency, this simulation shows that there is no significant change in mP values in both mechanisms when the signal amplitude $\gamma > \sim 6$. However, mP values decrease significantly in both mechanisms for the signal profiles with a fixed signal amplitude γ as the persistency parameter k increases. On the other hand, the simulations predict no significant difference in mT and D values. For this signal profile, mT value calculated for mechanism I_{md+} is 29 minutes, whereas it is calculated as 36 minutes for the mechanism I_{ms-} . Interestingly for the persistent signal $k = 100$, as the signal amplitude γ increases, the mT metric decreases in mRNA degradation mechanism I_{md+} , but not in the protein synthesis mechanism I_{ms-} . This is probably due to the fact that in our model the mRNA synthesis term is constant but the mRNA degradation term is linear. In the

solution for these models, the mRNA synthesis term changes the P levels linearly in time, and the degradation term affects the P levels exponentially in time. Hence, slowing down the mRNA synthesis rate reduces the protein production linearly without changing mT level significantly in mechanism I_{ms-} . On the other hand, mechanism I_{md+} reduces the protein synthesis levels exponentially, making the time to reach mid-protein level noticeably shorter.

4.2 Comparison of the Protein Control Mechanisms

We solved the models I_{pd+} (increased protein degradation) and I_{ps-} (decreased protein synthesis) numerically to study the effects of a transient signal on the protein abundance. Both mechanisms involve protein targeted regulations to decrease protein (P) levels in the cell but through distinct mechanisms. For persistent and high amplitude signals, our simulation results predict that I_{pd+} is slightly more effective in decreasing the levels of the protein than I_{ps-} (Figure 4A). In mechanism I_{pd+} , protein levels can decrease down to 263 molec/cell (~ 1.9 fold decrease from the steady state level), whereas in mechanism I_{ps-} protein levels decrease down to 295 molec/cell (~ 1.7 fold decrease from the steady state level). This simulation shows that mechanism I_{pd+} can decrease mP levels ~ 1.1 fold more than mechanism I_{ps-} . Moreover, mP dependency on the signal persistency and amplitude in mechanisms I_{pd+} and I_{ps-} is remarkably different (Figure 4A). Above a threshold value for signal amplitude of $\gamma = \sim 8$, I_{pd+} shows very little difference in mP levels for all signal persistency levels. But, mechanism I_{ps-} shows significant variation in mP levels as the signal persistency k varies for any fixed value of the signal amplitude γ . This suggests that changing the signal amplitude leads to higher variation in protein abundance in mechanism I_{ps-} , but not in mechanism I_{pd+} . For mechanism I_{pd+} , the lowest values of mP can be achieved with the signal amplitude values above ~ 8 and the signal persistency above ~ 20 minute, which suggests that the lowest values for mid-protein levels can be reached by a strong enough signal with any level of the signal persistency.

Mechanisms I_{pd+} and I_{ps-} qualitatively show vastly different dynamics in the mT metric as the signal persistency and signal amplitude change (Figure 4B). For the strong and persistent signal ($\gamma = 20$ and $k = 100$), the mT value is 2 min for mechanism I_{pd+} and 29 min for mechanism I_{ps-} , which is significantly longer. Above a threshold value of $\gamma = \sim 8$ for the signal amplitude, our simulation shows that there is no significant change in mT metric as k changes in mechanism I_{pd+} . On the other hand mechanism I_{ps-} shows a higher variation in this metric. Regarding the duration metric D , our simulation results show that the mechanisms I_{pd+} and I_{ps-} exhibit relatively similar qualitative behavior but slightly different quantitative behavior on the D metric (Figure 4C). While the duration D can go

up to 133 min in mechanism I_{pd+} , it goes only up to 108 minutes in mechanism I_{ps-} .

4.3 Comparison of the mRNA versus Protein Control Mechanisms

The mRNA and protein synthesis mechanisms (I_{ms-} and I_{ps-}) overall show qualitatively and quantitatively similar behavior. For a persistent and strong signal ($k = 100$ and $\gamma = 20$), mechanism I_{ms-} has mP levels of 299 molec/cell in average, while this value is 295 molec/cell for mechanism I_{ps-} (~ 1.7 fold decrease from steady state levels in both cases). The heat maps for the time required to reach the mid-protein abundance, mT , are also very similar for both mechanisms I_{ms-} and I_{ps-} (36 min and 29 min, respectively). This suggests that decreasing the rates of mRNA or protein synthesis results in similar mP and mT values, although mechanism I_{ps-} results in slightly lower mP values in a slightly shorter time. No significant difference is observed for the duration of the response, D , in both mechanisms.

In comparing the increased mRNA and protein degradation mechanisms (I_{md+} and I_{pd+}) for a strong and persistent signal profile, I_{pd+} is more efficient than I_{md+} . Mechanism I_{pd+} results in mP levels of 263 molec/cell whereas mechanism I_{md+} results in mP levels of 295 molec/cell (~ 1.9 and ~ 1.7 fold decreases from steady state level, respectively). Furthermore, the time to reach mid-protein levels is significantly shorter in mechanism I_{pd+} compared to I_{md+} (2 min and 29 min, respectively). The duration is longer for mechanism I_{pd+} (133 min) compared to I_{md+} (116 min).

4.4 Comparison of the Production versus Degradation Mechanisms

By looking at the simulations together, we observe that the mechanisms that increase mRNA and protein degradation (I_{md+} and I_{pd+}) are slightly more efficient than the mechanisms that decrease mRNA and protein synthesis (I_{ms-} and I_{ps-}). For the persistent and strong signal profile, the mP values computed for I_{md+} and I_{pd+} are respectively 295 molec/cell and 263 molec/cell. These values for I_{ms-} and I_{ps-} are 299 molec/cell and 295 molec/cell, respectively. Of all four mechanisms, I_{pd+} is the most efficient and I_{ms-} is the least efficient in the mP metric. This observation suggests that a system that needs lower levels of a certain protein should employ mechanism I_{pd+} rather than the other three mechanisms. Furthermore, for mechanism I_{pd+} , changes in the signal amplitude have almost no effect on the protein abundance when $\gamma > \sim 8$. The other mechanisms on the other hand, show greater dependence on the both parameters.

Our simulations predict that the heat maps for the mT metric are qualitatively and quan-

tatively similar for all mechanisms, except I_{pd^+} . In the I_{pd^+} mechanism, with a strong enough signal at any persistency, the mT metric reaches its minimum around 2 minutes, which is much longer for the other three mechanisms (29-36 minutes). Hence, systems that need a quicker response may prefer mechanism I_{pd^+} , while long-term responses are better suited for the other three mechanisms. Finally, the duration for mechanism I_{pd^+} is 133 min, the longest of these four mechanisms.

5 The Stochastic Effects

The deterministic models only provide the average system dynamics and ignore effects of random fluctuations that are inherent in biological systems. Therefore, the deterministic approach may not accurately capture the true dynamics especially at low molecule numbers, as biochemical reactions in cells are inherently noisy processes[29, 30, 31]. To study cell-to-cell variation and roles of random fluctuations in regulations, we used stochastic simulations on the mechanisms A_j , ($j = md^-, ms^+, pd^-, ps^+$) and I_j , ($j = md^+, ms^-, pd^+, ps^-$). The Gillespie Algorithm is employed here to simulate the stochastic dynamics for all eight mechanisms using MatLab software.

To mimic a noisy system and perform the stochastic simulations, all the parameter values were held constant at the values listed in Section 2.3 except for α_p . We fixed this parameter at $\alpha_p = 0.5$, chose a strong and persistent signal ($\gamma = 20$ and $k = 100$) and stochastically simulated each of the systems for 600 min, which is long enough for the systems to reach their steady state. These values for the parameters result in a signal profile with the signal persistency of 100 minutes, the signal amplitude of 20, and a steady state protein molecule number of 100 molec/cell. This number falls in a range of experimentally measured protein numbers in *E. coli*[28]. A relatively small steady state level was selected to investigate effects of noise in the dynamics. For each mechanism, one thousand stochastic simulations were run until the system reaches a steady state after the removal of the signal. The results of the stochastic simulations are summarized below. To compare with the stochastic simulation results, we also numerically solved the deterministic models for this new parameter values as the signal amplitude γ changes between 1 and 20 and the signal persistency parameter k varies between 5 and 100 minutes. The results of the deterministic simulations are given in the supplementary section.

5.1 The Stochastic Effects in the Activation Mechanisms

The probability density functions for three response metrics from the stochastic simulations of the activation mechanisms A_{md-} (decrease mRNA degradation), A_{ms+} (increase mRNA synthesis), A_{pd-} (decrease protein degradation) and A_{ps+} (increase protein synthesis) are depicted in Figure 5. These mechanisms show different noise behaviors. The summary statistics for the activation mechanisms is listed in Table 3. To measure variation in these mechanisms, the coefficient of variation (CV) is used, which is defined as the ratio of the standard deviation (SD) and the mean of the distribution. The first graph in Figure 5 shows probability density for mP metric. Mechanism A_{md-} has a peak around 410 molec/cell with a standard deviation 52 molec/cell and a CV value of 12.7, which suggests that the most likely mid-protein level mP for this mechanism is around 410 molec/cell. Mechanism A_{ms+} has a larger and narrower peak around 951 molecules of protein per cell with a standard deviation 44.3 molec/cell and a CV value of 4.7, which suggests this mechanism is more likely to have greater mP levels. Mechanism A_{pd-} has the lowest mP values, with a very high and narrow peak around 193 molec/cell with a standard deviation 18.9 molec/cell and a CV value of 9.8. Finally, mechanism A_{ps+} has relatively short and broad peak around 1019 molec/cell, which is slightly higher than that of mechanism A_{ms+} , although the peak for A_{ps+} is much broader and shorter (with a standard deviation 179.9 molec/cell and CV value of 17.7), suggesting that there is a wider range in mP values and it has a lower probability at that value. Therefore, the mid-protein levels mP for these four mechanisms from least to greatest is as follows: A_{pd-} , A_{md-} , A_{ms+} , and A_{ps+} . But, in comparing the CV values, the order from least to most is as follows: A_{ms+} , A_{pd-} , A_{md-} and A_{ps+} . So, it is important to notice that although mechanism A_{ps+} results in the highest mP levels, this mechanism also shows the greatest variation, whereas mechanism A_{pd-} which shows the lowest mP has the second lowest deviation in mP . This simulation predicts that mechanisms A_{ms+} and A_{ps+} are the most effective in increasing mP levels, which is consistent with the results in Figure 3. Although these two mechanisms have comparable mid-protein levels, mechanisms A_{ms+} has four fold lower variation.

===== Figure 5 here =====

In the second graph in Figure 5 looking at the changes in probability density for mT metric, mechanisms A_{md-} , A_{pd-} and A_{ps+} have peaks hovering respectively around 63 min (with SD=5.8 min and CV=9.2), 50 min (with SD=9.7 min and CV=19.5) and 32 (with SD=12.1 min and CV=37.5) but the peak for mechanism A_{ms+} is the tallest and most narrow (with SD=3.1 min and CV=8.7). This suggests that mechanism A_{ms+} has the highest probability of having an mT value around 36 minutes. The peaks for mechanisms A_{ms+} and A_{ps+} show

slightly different mean mT values. However, mechanism A_{ps+} has higher variation. mT for mechanism A_{ps+} is the lowest of the four mechanisms with a shorter and wider peak around 32 minutes. This simulation shows that mechanism A_{ms+} responds to the signal quickest to reach the mid-protein level with the least variation.

The third graph, which maps out the probability density for the duration metric D , predicts that mechanism A_{ms+} has the highest value for the duration metric D , with a peak around 108 min. This mechanism also has the least variation of the four in this metric. Our simulations predict that mechanisms A_{pd-} and A_{ps+} have comparable short and wide peaks around 89 min and 99 min. Mechanism A_{md-} has a peak around 84 min that is comparable to mechanisms A_{pd-} and A_{ps+} in terms of mean D value but has a larger variation. According to our simulations, mechanism A_{ms+} proves to have the highest duration with the least variation in the simulation.

Table 3: The mean, standard deviation(SD) and coefficients of variation(CV) values for the three response metrics calculated from the stochastic simulations with 1000 runs for the activation mechanisms when $k = 100$, $\gamma = 20$ and $P^* = 100$.

	mP		mT		D	
	Mean \pm SD(molec/cell)	CV(%)	Mean \pm SD(min)	CV(%)	Mean \pm SD(min)	CV(%)
A_{md-}	410.3 \pm 52.0	12.7	63.1 \pm 5.8	9.2	83.601 \pm 7.1	8.5
A_{ms+}	950.7 \pm 44.3	4.7	35.5 \pm 3.1	8.7	107.83 \pm 3.8	3.5
A_{pd-}	193.0 \pm 18.9	9.8	49.6 \pm 9.7	19.5	88.539 \pm 14.3	16.2
A_{ps+}	1018.7 \pm 179.9	17.7	32.3 \pm 12.1	37.5	99.087 \pm 12.3	12.4

5.2 The Stochastic Effects in the Inhibition Mechanisms

For the inhibition mechanisms, I_{md+} (increase mRNA degradation), I_{ms-} (decrease mRNA synthesis), I_{pd+} (increase protein degradation) and I_{ps-} (decrease protein synthesis), the probability density functions for the three response metrics produced from our stochastic simulations are given in Figure 6. As seen, these mechanisms show different stochastic characteristics. The summary of the statistics for the response metrics of the inhibition mechanisms is tabulated in Table 4.

In the first graph in Figure 6, the probability density functions are depicted for the mP metric. The peak for mechanism I_{pd+} is strikingly different than the peaks for the other three mechanisms. This mechanism attains a mid-protein level mP around 50 molec/cell with a standard deviation of 0.2 molec/cell and a CV value of 0.4. The other three mechanisms display similar peaks around 58 molec/cell with relatively similar variations. The standard deviations calculated for I_{md+} , I_{ms-} and I_{ps-} are 2, 2.6 and 2 molec/cell, respectively.

The CV values calculated for these 3 mechanisms are respectively 3.4, 4.5 and 3.4. Our simulations show that these 3 mechanisms do not result in mP values that are significantly different. This is in agreement with the results observed in Figure S.2, where mechanism I_{pd+} has slightly lower values for mP compared to the other three mechanisms. Although mechanisms I_{md+} , I_{ms-} and I_{ps-} display slightly higher mP levels, they also display larger deviation than mechanism I_{pd+} . Therefore, a system that requires a more precise decrease in mP should employ mechanism I_{pd+} , but systems where noise is beneficial may use any of the other three mechanisms.

===== Figure 6 here =====

The middle graph in Figure 6 shows the probability density function for mT . Mechanism I_{pd+} displays significantly lower values for mT , with an average peak around 2 min, the standard deviation of .3 min and a CV value of 15.9. Mechanisms I_{md+} and I_{ps-} have similar peaks around 30 min with very similar levels of variation. The CV values calculated for I_{md+} and I_{ps-} are 16 and 15.7, respectively. Mechanism I_{ms-} is a little slower, with a peak around 36 min but has relatively similar variation to the other mechanisms. The CV value calculated for I_{ms-} is 18.3. Overall, mechanism I_{pd+} is the quickest of the four and shows the second lowest variation with a CV value of 15.9. Therefore, systems that require a fast and precise response should employ mechanism I_{pd+} .

The last graph in Figure 6 shows probability density function for the duration metric D . Mechanisms I_{md+} , I_{ms-} and I_{ps-} show very similar duration with values around 122 min (SD=23.4 min and CV=19.1), 117 min (SD=23.4 min and CV=20) and 115 min (SD=23.2 min and CV=20.1). Consistent with the previous two metrics, the peak for mechanism I_{pd+} is slightly different, with a value of about 137 min (SD=18.7 min and CV=13.7).

Table 4: The mean, standard deviation(SD) and coefficients of variation(CV) values for the three response metrics calculated from the stochastic simulations with 1000 runs for the inhibition mechanisms when $k = 100$, $\gamma = 20$ and $P^* = 100$.

	mP		mT		D	
	Mean \pm SD(molec/cell)	CV(%)	Mean \pm SD(min)	CV(%)	Mean \pm SD(min)	CV(%)
I_{md+}	58.1 \pm 2.0	3.4	30.0 \pm 4.8	16.0	122.3 \pm 23.4	19.1
I_{ms-}	58.5 \pm 2.6	4.5	36.4 \pm 6.7	18.3	117.1 \pm 23.4	20.0
I_{pd+}	50.1 \pm 0.2	0.4	1.8 \pm 0.3	15.9	137.0 \pm 18.7	13.7
I_{ps-}	58.3 \pm 2.0	3.4	29.1 \pm 4.6	15.7	115.4 \pm 23.2	20.1

5.3 Noise Dynamics

In this section, we studied how stochasticity changes as a function of time for both the activation and the inhibition mechanisms. The stochastic simulations were run as described above and the coefficient of variation (CV) values are calculated every 6 minutes, and the results are displayed in Figure 7.

Among the activation mechanisms, A_{md-} peaks around 30 minutes with a CV about 0.17, mechanism A_{ms+} peaks around 10 minutes with a CV about 0.085, mechanism A_{pd-} peaks around 50 minutes with a CV about 0.13 and remains at that level until around 170 minutes, and mechanism A_{ps+} peaks around 20 minutes with a CV about 0.3. In the first ~ 300 minutes, mechanism A_{ms+} has the least noise. On the other hand, mechanism A_{ps+} has the most noise in the first 200 minutes. Although the noise levels starts declining after the peak value the levels remain higher than the other mechanisms until about 200 minutes. Mechanisms A_{md-} and A_{pd-} display similar noise dynamics, but A_{pd-} has slightly less noise than A_{md-} for the first 150 minutes. Interestingly, at 150 min there is a switch and mechanism A_{pd-} becomes noisier after 150 min. Remarkably, only mechanism A_{ps+} has noise level that rise above the steady state noise level. At the steady state, all four mechanisms have similar stochasticity.

===== Figure 7 here =====

In considering these results with the function of each mechanism, there are some interesting observations to note. Mechanism A_{ms+} , which showed the lowest noise levels, represents a signal to increase mRNA synthesis. It seems that a system that functions best in low noise conditions would employ this mechanism. In contrast, mechanism A_{ps+} , which results in an increased protein synthesis rate, showed the highest noise levels prior to 200 minutes. It is also interesting to notice that A_{md-} and A_{pd-} , the mechanisms that result in decreased mRNA and protein degradation respectively, have very similar noise levels, although mechanism A_{md-} exhibits slightly higher initial noise levels.

The next graph shows the noise levels of the four inhibition mechanisms. Mechanisms I_{md+} and I_{ps-} show similar noise level dynamics, whereas mechanisms I_{ms-} and I_{pd+} show different noise level dynamics. In the first 200 minutes, mechanism I_{pd+} has the highest noise levels, which peak very early (around 10 minutes) and stay roughly constant until 100 minutes, with a CV of about 0.55. The other three mechanisms slowly rise and don't peak until around 150 minutes, but with very similar CV values (~ 0.3). Mechanisms I_{md+} and I_{ps-} show similar variation throughout time, while mechanism I_{pd+} displays significantly higher noise levels in comparison to these two mechanisms in the first 150 minutes. After 150 minutes all four mechanisms' noise levels decrease and around 300 minutes they reach a steady-state. A

system that requires low noise conditions over time should employ mechanism I_{md+} (signal to increase mRNA degradation) or I_{ps-} (signal to decrease protein synthesis), as those two mechanisms exhibited the least noise. It is interesting to see that mechanisms I_{md+} and I_{ps-} show very similar noise levels throughout the time-course, because these two mechanisms are acting in different ways (increased mRNA degradation versus decreased protein synthesis). A system that benefits from noise should employ mechanism I_{pd+} as this mechanism was the noisiest of the four inhibition mechanisms. Interestingly before reaching a steady state level, all mechanisms have noise levels that rise temporarily above the steady state noise level, but mechanism I_{pd+} is much noisier.

6 Discussions

Using deterministic and stochastic methods, we analyzed the responses produced by four activation and four inhibition mechanisms on the protein abundance triggered by a transient signal at both population and single cell levels. The responses are measured by three metrics. With the help of the deterministic models which involve differential equations, the average behavior of the protein dynamics was studied at the population level. The single cell dynamics and cell-to-cell variation were studied by a stochastic method employing the Gillespie algorithm. Our deterministic simulations showed that the protein levels in mechanisms A_{ms+} or A_{ps+} are higher compared to the protein levels in mechanisms A_{md-} and A_{pd-} for approximately same signal profile. This suggests that a biological system that needs high levels of a certain protein should employ either mechanism A_{ms+} or A_{ps+} rather than mechanisms A_{md-} and A_{pd-} . Our simulations also predict that the time required to reach to the mid-protein level mP is slightly faster in both mechanisms A_{ms+} and A_{ps+} . Hence, biological systems that need a quicker response may prefer either mechanisms A_{ms+} or A_{ps+} , while systems that require slower responses are better suited for mechanisms A_{md-} or A_{pd-} . Of the four activation mechanisms, our deterministic simulations predict that mechanism A_{ps+} results in the highest mP level in quickest time, mT . The stochastic simulations showed that among the four activation mechanisms, mechanisms A_{ms+} and A_{ps+} show the least and the most variations for the response metrics mP and mT , respectively. Hence, systems that need low-noise situations should employ mechanism A_{ms+} .

Mechanism A_{ps+} has the architecture that most directly affects the protein abundance. This mechanism is employed by biological systems such as MAPK signaling. Ras signaling pathway activates downstream MAP kinases that phosphorylate protein eIF4E and results in an increase in the protein synthesis [32]. A system that requires a fast and large increase

in protein abundance should employ this mechanism. On the other hand, mechanism A_{ms+} , which results in protein abundance similar to mechanism A_{ps+} , shows the least variation in both mP and mT metrics. Mechanism A_{ms+} is observed in biological systems such as TGF-beta signaling. In this pathway, when the ligand binds to the receptor, downstream Smad proteins are phosphorylated and can interact with coactivators to increase transcription of target genes[33]. Although mechanisms A_{md-} and A_{pd-} resulted in lower mP levels in a longer period of time, some systems may employ these mechanisms depending on the conditions and the cellular needs. Kassel *et al.*[34] found that glucocorticoids act to reduce degradation of MKP-1, which results in inhibition of the downstream target gene ERK-1/2. Interestingly, glucocorticoids also increase transcription of MKP-1, which suggests that a system will likely employ different mechanisms in combination to achieve the desired effect. Mechanism A_{md-} seems to also be found in gene regulatory networks. One method of mRNA degradation is deadenylation of the poly-A tail and degradation by a form of exonuclease [35, 16], and the decrease in mRNA degradation is related to decreased activity of deadenylase enzymes, thus increasing mRNA stability.

Of the four inhibition mechanisms, mechanism I_{pd+} (signal dependent increase in protein degradation) results in slightly lower mP and significantly reduced mT levels in our deterministic simulations. On the other hand, in the stochastic simulations, this mechanism results in the least variation in mP metric among the four inhibition mechanisms. According to the noise dynamics simulation, it has the most noise prior to 200 minutes (see Figure 7).

The degradation of proteins is the most direct way to reduce protein levels, as it is closest to the final product, whereas mRNA degradation for example is a process further upstream of protein synthesis and degradation. Protein ubiquitination, a means of degradation, is performed by the enzyme 26S proteasome[36]. Bile acid signaling prevents degradation of Small Heterodimer Partner(SHP-a protein involved in bile acid signaling) by inhibiting ubiquitin proteasomal degradation. However, this protein is targeted for degradation by a ubiquitination process in other circumstances [37, 38].

Mechanisms I_{md+} and I_{ps-} showed identical mP levels and similar mT values in the deterministic simulations. These two mechanisms also displayed very similar noise dynamics in the stochastic simulations. On the other hand, mechanism I_{ms-} is slightly less effective and the slowest of the four inhibition mechanisms(Figure 4). In the stochastic simulations this mechanism shows similar mP values with mechanisms I_{md+} and I_{ps-} , but higher variation. A good example for mechanism I_{md+} is the protein BRF1, which is important in mRNA degradation via AU-rich element mediated decay [39], is phosphorylated by MK2, activating its mRNA degrading activity [38]. On the other hand, an example for mechanism I_{ms-} is

seen in the MAPK signaling pathway. In this pathway, Ras activates transcription factors that block the expression of downstream target genes, resulting in reduced apoptosis [40]. Hence, each mechanism, although having various levels of effectiveness and quickness, is shown to be employed by cells in different circumstances.

Taken together, it is clear that biological systems use these mechanisms in combination with one another to increase or decrease protein abundance at different time scales and durations. This gives rise to the great complexity within gene regulation in biology. This study sheds light on why cells might have evolved to use certain mechanisms more than others depending on the protein levels required and the time constraints. It also provides the opportunity to look in a more detailed way at the efficacy of gene regulation at mRNA and protein production levels, which helps understand why a certain biological system prefers a specific mode of increasing or decreasing protein expression depending on the needs of cells and specific environmental conditions. Here we developed mathematical models that can compare these mechanisms in terms of mid-protein levels, time required to reach mid-protein levels, and the duration of the response. In future studies it would be interesting to pair this kind of study with biological experiments to more closely examine which environmental conditions favor the use of one mechanism over another.

Acknowledgment:

We thank members of the Ay and Yildirim laboratories for their comments. This work was partially supported by the Carter Wallace Fellowship to Prof. Ahmet Ay and the New College of Florida Faculty Development Fund to Prof. Necmettin Yildirim.

References

- [1] Crick F, et al. Central dogma of molecular biology. *Nature*. 1970;227(5258):561–563.
- [2] Zhang Y, Reinberg D. Transcription regulation by histone methylation: interplay between different covalent modifications of the core histone tails. *Genes & development*. 2001;15(18):2343–2360.
- [3] Forsythe JA, Jiang BH, Iyer NV, Agani F, Leung SW, Koos RD, et al. Activation of vascular endothelial growth factor gene transcription by hypoxia-inducible factor 1. *Molecular and cellular biology*. 1996;16(9):4604–4613.
- [4] Zheng Wp, Flavell RA. The transcription factor GATA-3 is necessary and sufficient for Th2 cytokine gene expression in CD4 T cells. *Cell*. 1997;89(4):587–596.

- [5] Libermann TA, Baltimore D. Activation of interleukin-6 gene expression through the NF-kappa B transcription factor. *Molecular and cellular biology*. 1990;10(5):2327–2334.
- [6] Mapp AK, Ansari AZ, Ptashne M, Dervan PB. Activation of gene expression by small molecule transcription factors. *Proceedings of the National Academy of Sciences*. 2000;97(8):3930–3935.
- [7] Lemon B, Tjian R. Orchestrated response: a symphony of transcription factors for gene control. *Genes & development*. 2000;14(20):2551–2569.
- [8] Kwak H, Lis JT. Control of transcriptional elongation. *Annual review of genetics*. 2013;47:483.
- [9] Sims RJ, Belotserkovskaya R, Reinberg D. Elongation by RNA polymerase II: the short and long of it. *Genes & development*. 2004;18(20):2437–2468.
- [10] Proudfoot NJ, Furger A, Dye MJ. Integrating mRNA processing with transcription. *Cell*. 2002;108(4):501–512.
- [11] Wilusz CJ, Wormington M, Peltz SW. The cap-to-tail guide to mRNA turnover. *Nature Reviews Molecular Cell Biology*. 2001;2(4):237–246.
- [12] Komarnitsky P, Cho EJ, Buratowski S. Different phosphorylated forms of RNA polymerase II and associated mRNA processing factors during transcription. *Genes & development*. 2000;14(19):2452–2460.
- [13] Edmonds M, Abrams R. Polynucleotide biosynthesis: formation of a sequence of adenylylate units from adenosine triphosphate by an enzyme from thymus nuclei. *Journal of Biological Chemistry*. 1960;235(4):1142–1149.
- [14] Beelman CA, Parker R. Degradation of mRNA in eukaryotes. *Cell*. 1995;81(2):179–183.
- [15] Garneau NL, Wilusz J, Wilusz CJ. The highways and byways of mRNA decay. *Nature reviews Molecular cell biology*. 2007;8(2):113–126.
- [16] Valencia-Sanchez MA, Liu J, Hannon GJ, Parker R. Control of translation and mRNA degradation by miRNAs and siRNAs. *Genes & development*. 2006;20(5):515–524.
- [17] Hochstrasser M. Ubiquitin-dependent protein degradation. *Annual review of genetics*. 1996;30(1):405–439.

- [18] Goldberg AL. Protein degradation and protection against misfolded or damaged proteins. *Nature*. 2003;426(6968):895–899.
- [19] Alon U. Network motifs: theory and experimental approaches. *Nat Rev Genet*. 2007 Jun;8(6):450–461.
- [20] Çağatay T, Turcotte M, Elowitz MB, Garcia-Ojalvo J, Süel GM. Architecture-dependent noise discriminates functionally analogous differentiation circuits. *Cell*. 2009;139(3):512–522.
- [21] Wall ME, Hlavacek WS, Savageau MA. Design of gene circuits: lessons from bacteria. *Nature Reviews Genetics*. 2004;5(1):34–42.
- [22] Savageau MA. Design principles for elementary gene circuits: Elements, methods, and examples. *Chaos: An Interdisciplinary Journal of Nonlinear Science*. 2001;11(1):142–159.
- [23] Ay A, Yildirim N. Dynamics matter: differences and similarities between alternatively designed mechanisms. *Molecular BioSystems*. 2014;10(7):1948–1957.
- [24] Bernstein JA, Lin PH, Cohen SN, Lin-Chao S. Global analysis of *Escherichia coli* RNA degradosome function using DNA microarrays. *Proceedings of the National Academy of Sciences of the United States of America*. 2004;101(9):2758–2763.
- [25] Taniguchi Y, Choi PJ, Li GW, Chen H, Babu M, Hearn J, et al. Quantifying *E. coli* proteome and transcriptome with single-molecule sensitivity in single cells. *Science*. 2010;329(5991):533–538.
- [26] So Lh, Ghosh A, Zong C, Sepúlveda LA, Segev R, Golding I. General properties of transcriptional time series in *Escherichia coli*. *Nature genetics*. 2011;43(6):554–560.
- [27] Wong P, Gladney S, Keasling JD. Mathematical model of the *lac* operon: Inducer exclusion, catabolite repression, and diauxic growth on glucose and lactose. *Biotechnol Prog*. 1997;13:132.143.
- [28] Ishihama Y, Schmidt T, Rappsilber J, Mann M, Hartl FU, Kerner M, et al. Protein abundance profiling of the *Escherichia coli* cytosol. *BMC Genomics*. 2008;9(1):102.
- [29] Kepler TB, Elston TC. Stochasticity in transcriptional regulation: origins, consequences, and mathematical representations. *Biophysical journal*. 2001;81(6):3116–3136.

- [30] Wang X, Hao N, Dohlman HG, Elston TC. Bistability, stochasticity, and oscillations in the mitogen-activated protein kinase cascade. *Biophysical journal*. 2006;90(6):1961–1978.
- [31] Kærn M, Elston TC, Blake WJ, Collins JJ. Stochasticity in gene expression: from theories to phenotypes. *Nature Reviews Genetics*. 2005;6(6):451–464.
- [32] Holland EC, Sonenberg N, Pandolfi PP, Thomas G. Signaling control of mRNA translation in cancer pathogenesis. *Oncogene*. 2004;23(18):3138–3144.
- [33] Massagué J, Chen YG. Controlling TGF- β signaling. *Genes & development*. 2000;14(6):627–644.
- [34] Kassel O, Sancono A, Krätzschmar J, Kreft B, Stassen M, Cato AC. Glucocorticoids inhibit MAP kinase via increased expression and decreased degradation of MKP-1. *The EMBO Journal*. 2001;20(24):7108–7116.
- [35] Parker R, Song H. The enzymes and control of eukaryotic mRNA turnover. *Nature structural & molecular biology*. 2004;11(2):121–127.
- [36] Lecker SH, Goldberg AL, Mitch WE. Protein degradation by the ubiquitin–proteasome pathway in normal and disease states. *Journal of the American Society of Nephrology*. 2006;17(7):1807–1819.
- [37] Miao J, Xiao Z, Kanamaluru D, Min G, Yau PM, Veenstra TD, et al. Bile acid signaling pathways increase stability of Small Heterodimer Partner(SHP) by inhibiting ubiquitin–proteasomal degradation. *Genes & development*. 2009;23(8):986–996.
- [38] Maitra S, Chou CF, Lubber CA, Lee KY, Mann M, Chen CY. The AU-rich element mRNA decay-promoting activity of BRF1 is regulated by mitogen-activated protein kinase-activated protein kinase 2. *Rna*. 2008;14(5):950–959.
- [39] Chen CYA, Shyu AB. AU-rich elements: characterization and importance in mRNA degradation. *Trends in biochemical sciences*. 1995;20(11):465–470.
- [40] Kurada P, White K. Ras Promotes Cell Survival in *Drosophila* by Downregulating *hid* Expression. *Cell*. 1998;95(3):319–329.

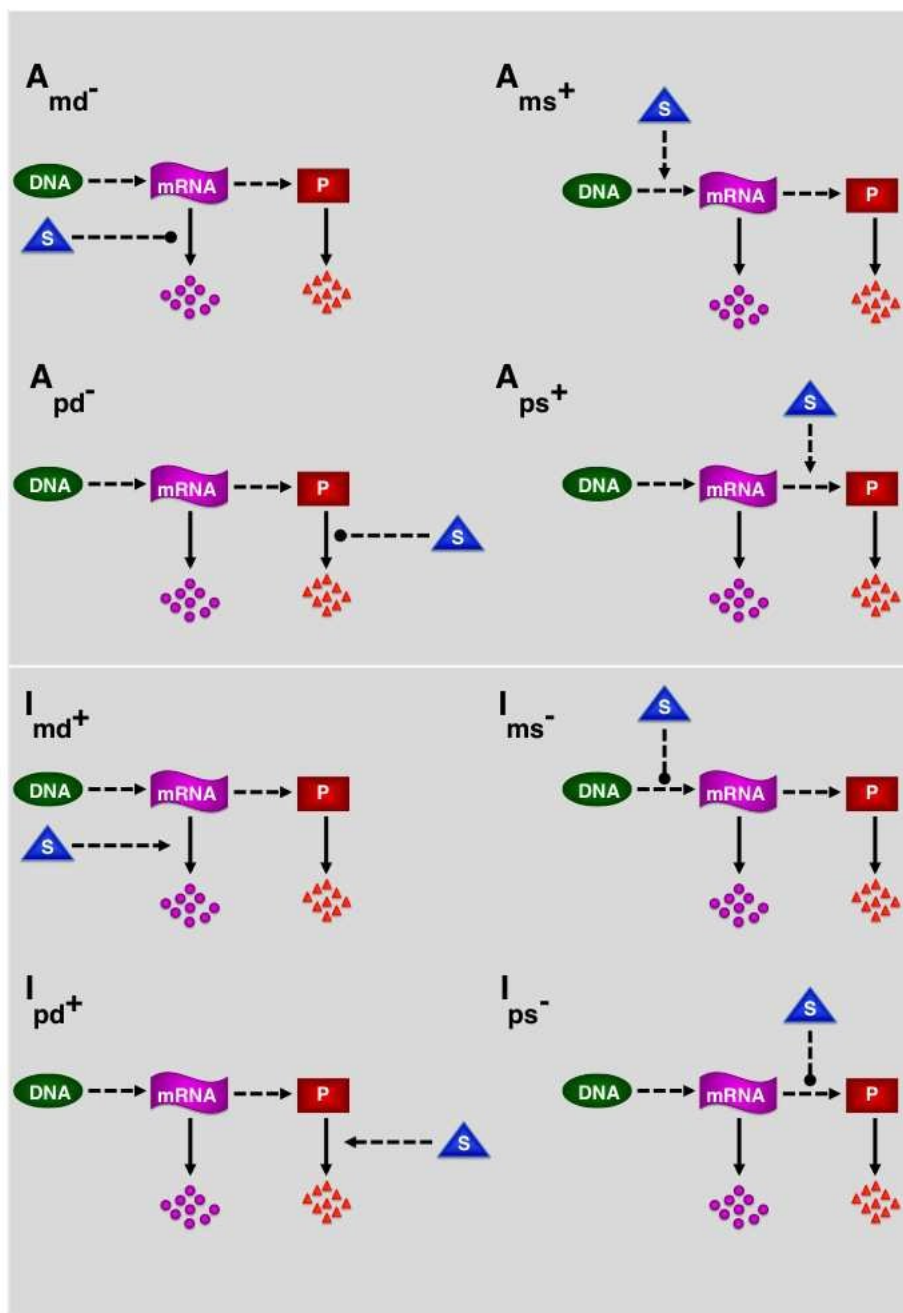


Figure 1: A cartoon depiction of four activation mechanisms A_{md^-} , A_{ms^+} , A_{pd^-} , and A_{ps^+} and four inhibition mechanisms I_{md^+} , I_{ms^-} , I_{pd^+} , and I_{ps^-} . The vertical and horizontal dotted lines with arrows directed towards another arrow are for the signal dependent increase in the synthesis or degradation. The vertical and horizontal dotted lines with rounded ends show the inhibition in the degradation or synthesis. The vertical solid lines with arrows show the degradation of the mRNA or the protein and horizontal dotted lines with arrows between DNA and mRNA or mRNA and protein represent the mRNA and protein synthesis, respectively.

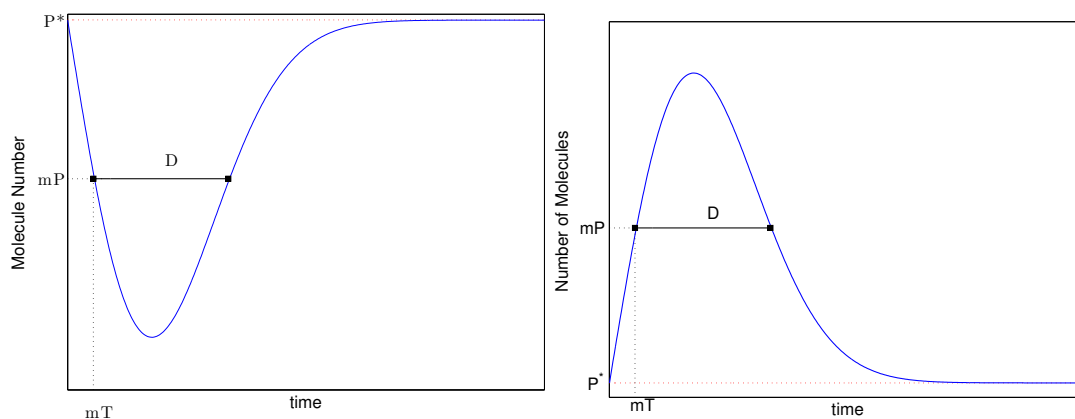


Figure 2: The graphical representation of the response metrics for the protein abundance for the inhibition (left) and activation (right) mechanisms after the disturbance of the system by a signal. The response metrics used to characterize the temporal changes in the protein abundance are the mid-protein abundance (mP), time required to reach mP level (mT) and the duration of response (D) are shown.

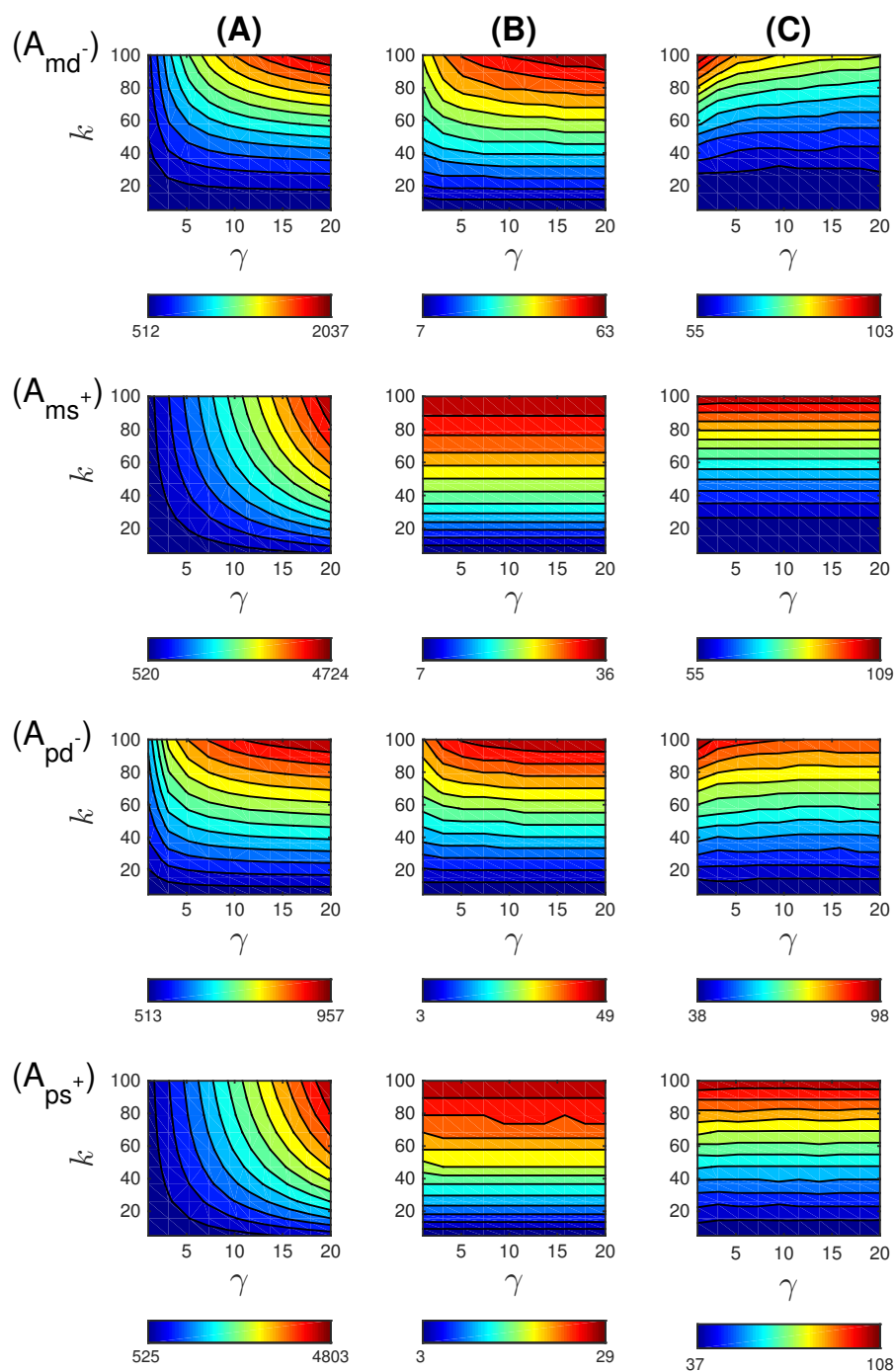


Figure 3: The dynamics of A_{md^-} , A_{ms^+} , A_{pd^-} and A_{ps^+} mechanisms when changing the signal profile with an amplitude γ ranging from a 1-fold to a 21-fold change and the signal persistency k ranging from 5 to 100 minutes. Increasing the signal amplitude results in ~ 2.3 fold difference in the mid-protein mP levels between mechanisms A_{md^-} and A_{ms^+} (column A). Mechanism A_{ps^+} showed the highest mP abundance (4803 molec/cell) and compared to mechanism A_{pd^-} which showed the lowest mP abundance (957 molec/cell) there is ~ 5.0 fold difference (column A). The shortest time to reach mP levels was achieved by mechanism A_{ps^+} (29 min) and mechanism A_{md^-} showed the highest value for mT at 63 min (column B). Very little difference in the duration is observed in all four mechanisms (column C).

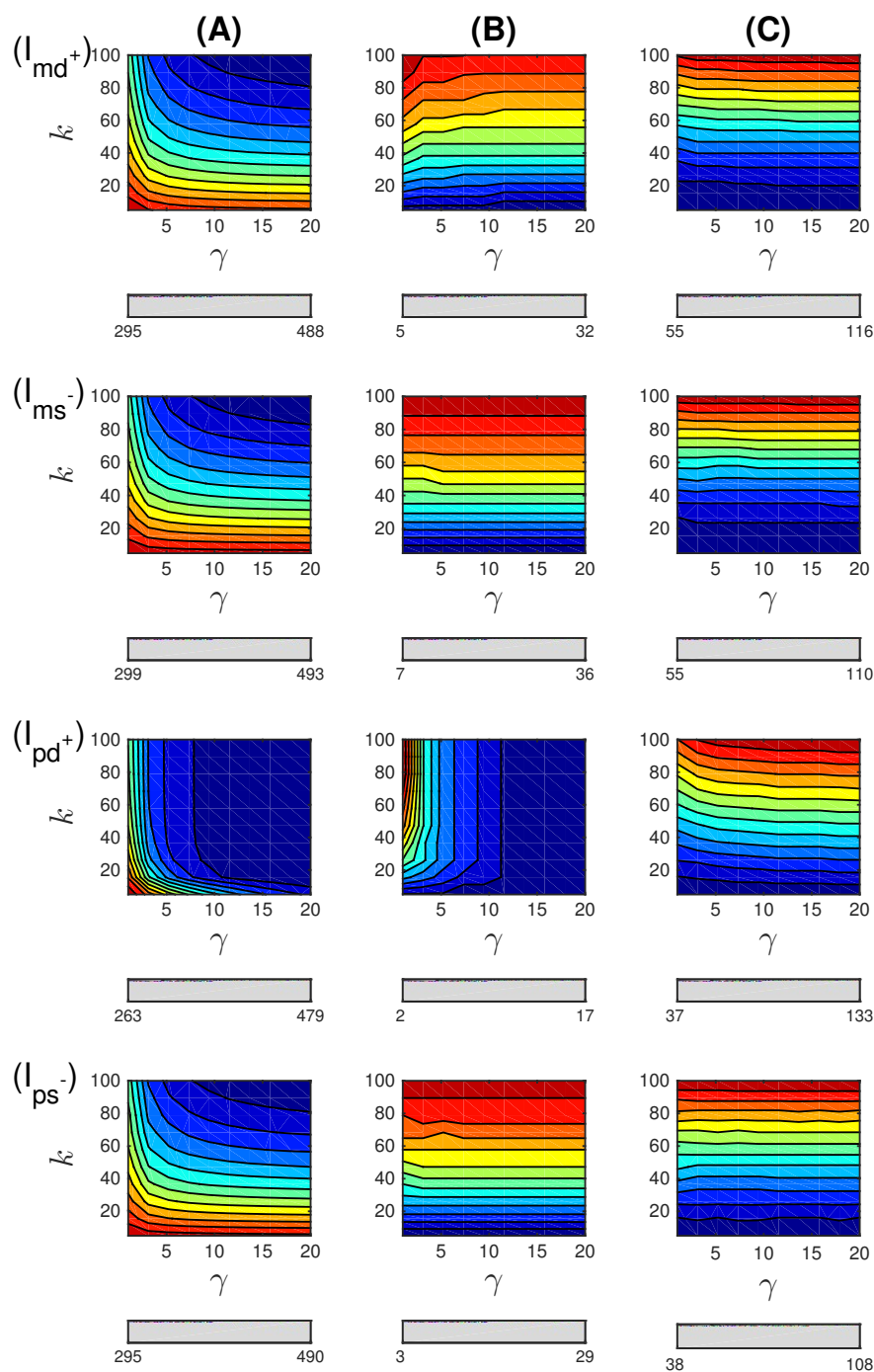


Figure 4: The dynamics of I_{md+} , I_{ms-} , I_{pd+} and I_{ps-} mechanisms and characteristics when changing the signal profile with the amplitude γ ranging from a 1-fold to a 21-fold change and the signal persistency k ranging from 5 to 100 minutes. Increasing the signal amplitude has a significant impact on the mid-protein mP levels in I_{md+} , I_{ms-} and I_{ps-} (column A). Overall, mechanism I_{pd+} shows the lowest mP level (263 molec/cell) and mechanism I_{ms-} shows the highest mP level (299 molec/cell) (column A). The fastest time to reach mP level is achieved by mechanism I_{pd+} (~ 2 min) and mechanism I_{ms-} is the slowest with an mT value of 36 min (column B). Little difference in the duration is observed in all four mechanisms (column C).

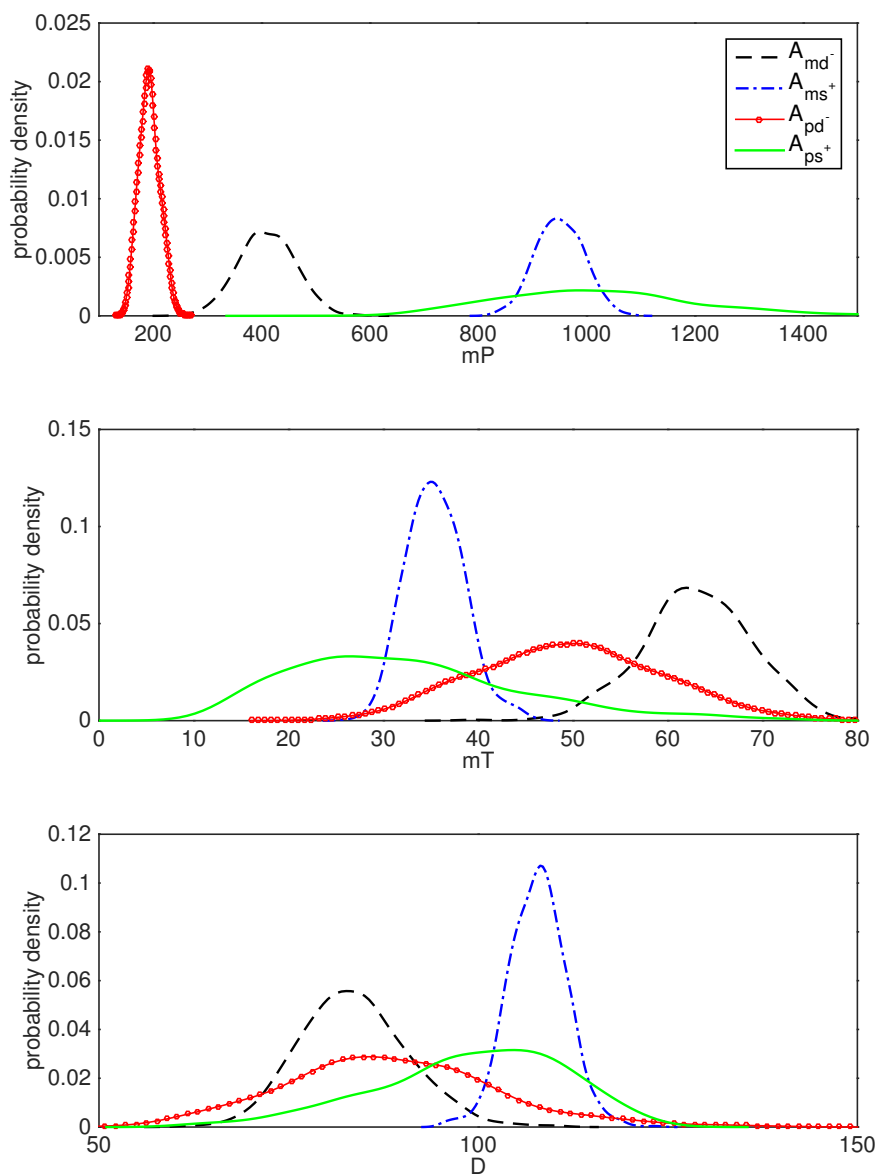


Figure 5: The probability density functions(pdf) for each metric are shown for the activation mechanisms. They display distinct characteristics. The top figure depicts the pdf for the metric mP . As seen in the figure, all mechanisms have different mean and standard deviations. A_{pd^-} has the smallest mean and standard deviation, but A_{ms^+} has the lowest coefficient of variation (Table 3). The middle figure represents the pdf for the metric mT . The mean mT values are higher for mechanisms A_{md^-} and A_{pd^-} in comparison to mechanisms A_{ms^+} and A_{ps^+} . A_{ms^+} has smaller standard deviation and variation in comparison to other mechanisms. The bottom figure shows the pdf for the duration metric D . A_{md^-} and A_{pd^-} have roughly same mean D , but A_{md^-} has the smaller standard deviation and variation in this metric. A_{ms^+} has the largest mean value for D with a small standard deviation and the coefficient of variation, and A_{ps^+} has a large mean value with a large standard deviation and a coefficient of variation.

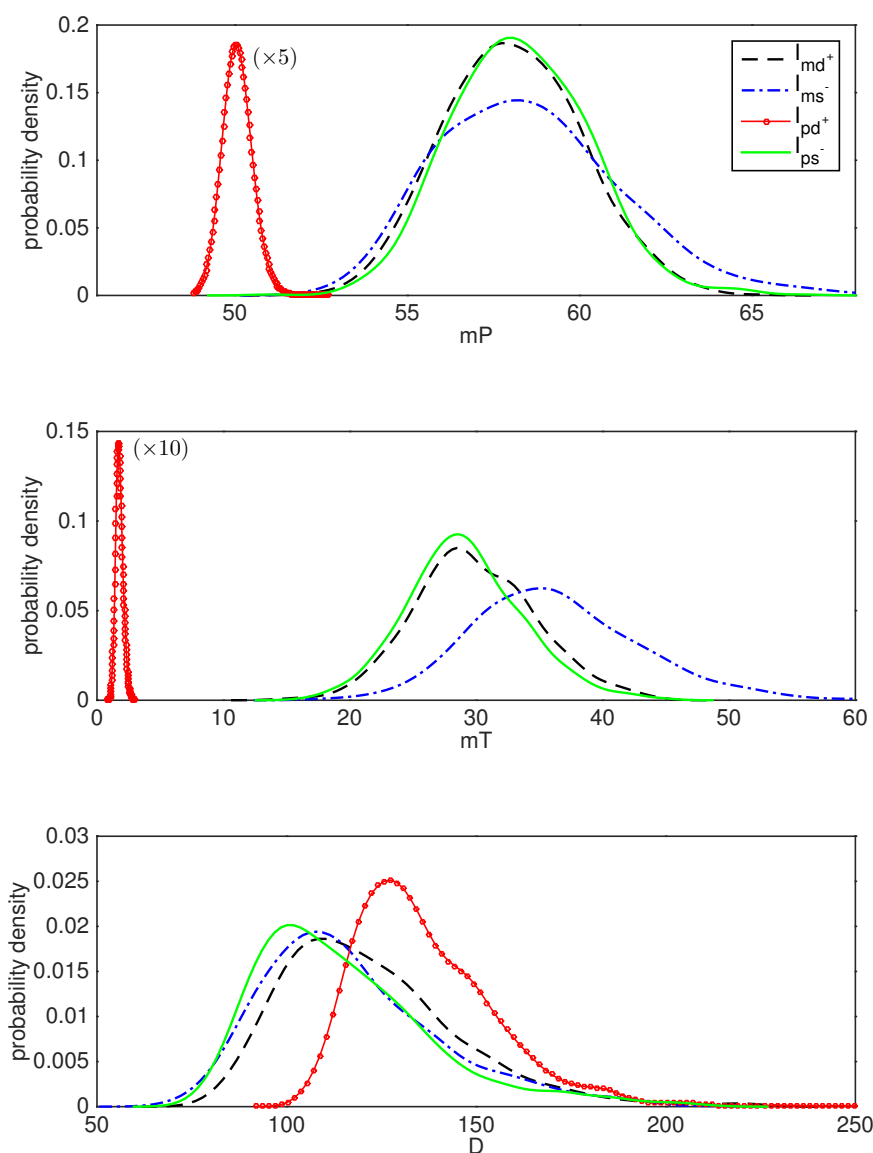


Figure 6: The probability density functions (pdf) for the three metrics for the inhibitory mechanisms are shown. The top figure depicts the pdf for mP . As seen in this figure, the mean mP values are roughly same for all mechanisms except I_{pd+} , which has the smallest standard deviation and the least variation (Table 4). Within the three mechanisms with similar mean mP values, I_{md+} and I_{ps-} have smaller standard deviations compared to I_{ms-} . The middle figure is the pdf for mT . The mean mT values are roughly same for mechanisms I_{md+} and I_{ps-} . Mechanism I_{ms-} shows slightly larger mT value and mechanism I_{pd+} has significantly smaller mean mT value. I_{md+} and I_{ps-} have smaller standard deviations when compared to I_{ms-} . The bottom figure shows the probability density function for the duration metric D . In regards to D , I_{md+} , I_{ms-} and I_{ps-} have roughly same mean and standard deviation. I_{pd+} has larger mean value with a smaller standard deviation and the coefficient of variation.

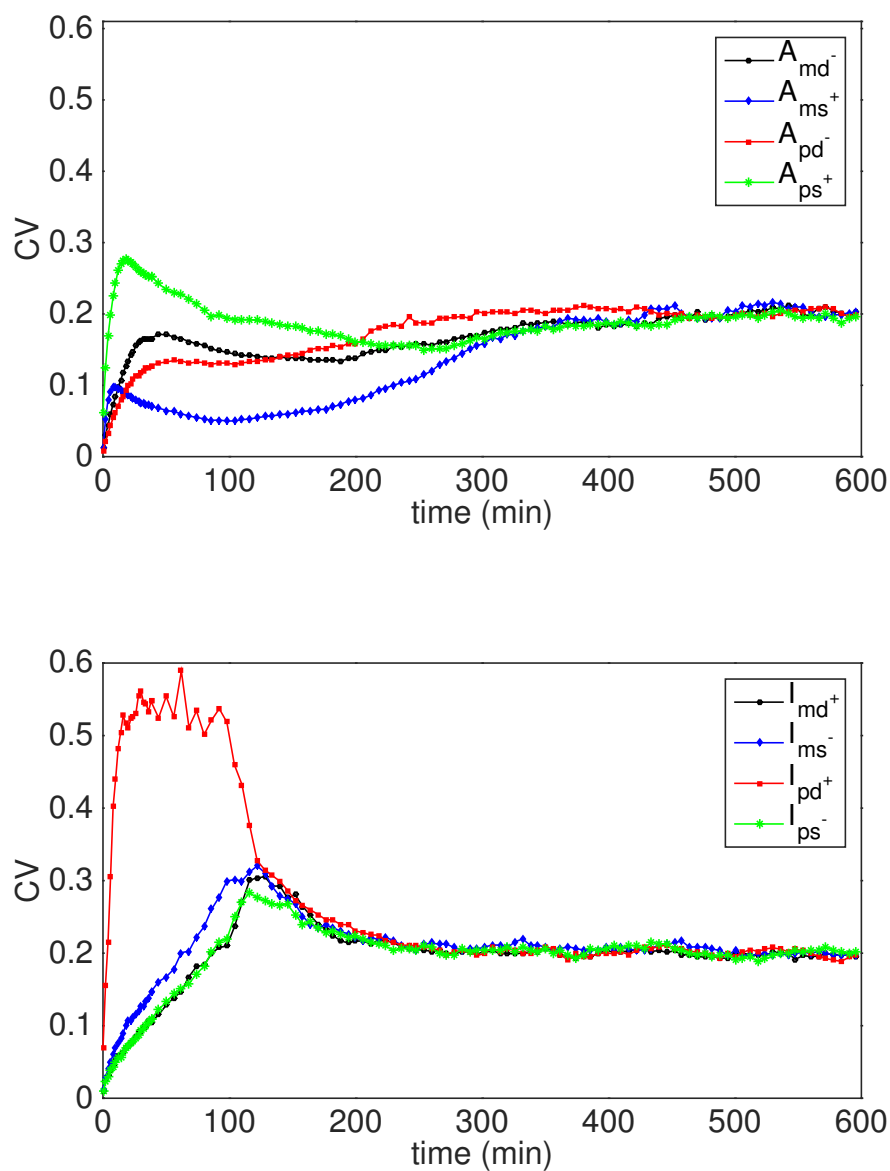


Figure 7: The coefficient of variations as a function of time for all the activatory and inhibitory mechanisms. The top figure depicts the coefficient of variations for the activation mechanisms. All mechanisms have different coefficient of variation over time before they reach to the same steady state level. The bottom figure displays the coefficient of variations for the inhibition mechanisms. As seen in the figure, mechanisms I_{md^+} and I_{ps^-} have similar coefficient of variation(CV) dynamics, while I_{ms^-} has slightly different and larger CV values, and I_{pd^+} shows the greatest difference in noise dynamics compared to the other three mechanisms.